Near-Infrared Spectroscopy

9

Byoung-joo Choi

Nowadays, various newly developed intracoronary imaging techniques have provided unique information on the coronary plaque and are widely used either for clinical decision-making or for research purposes (Table 9.1). However, there is still unmet need for the characterization of atheromatous plaque, especially for in vivo measurement of lipid burden within coronary artery wall. Near-infrared spectroscopy (NIRS) uses properties of the light reflection and absorption in each specific chemical component and provides us information on the presence of lipid core plaque in the coronary artery wall. This chapter will review the basic mechanism, validation, and techniques of NIRS followed by the results of early clinical studies.

Table 9.1 Comparison of different intravascular imaging modalities

Imaging modality	Resolution	Cap thickness	Lipid core	Calcium	Thrombus	Macrophage	Neovascularization
IVUS	100 μm	+	+	++	+	−	−
OCT	10 μm	+++	++	++	++	+	++
VH	100 μm	+	+	++	+	−	−
NIRS	−	+	+++	−	−	−	−
Angioscopy	−	+	+	−	+++	−	−

IVUS intravascular ultrasound, *OCT* optical coherence tomography, *VH* virtual histology, *NIRS* near-infrared spectroscopy

B.-j. Choi
Department of Cardiology, Ajou University School of Medicine, Suwon, South Korea
e-mail: bjchoi@ajou.ac.kr

M.-K. Hong (ed.), *Coronary Imaging and Physiology*,
https://doi.org/10.1007/978-981-10-2787-1_9

9.1 Basic Mechanism

Spectroscopy is well established and widely accepted method to identify unknown chemicals in a variety of industries and scientific studies. Basically, spectroscopy employs the mechanism that light reflection (scattering) and absorption vary at different wavelengths according to each chemical component or substance [1, 2]. Organic component in the atheromatous plaque (collagen, cholesterol, etc.), when near-infrared (wavelength 780–2500 nm) light is shed on them, provides unique spectral signature (there are particular and specific peaks and trough patterns according to each chemical substances) that can be used as "chemical thumbprint" [3]. All these information are integrated with grayscale intravascular ultrasound (IVUS) images and displayed into a single picture (Fig. 9.1).

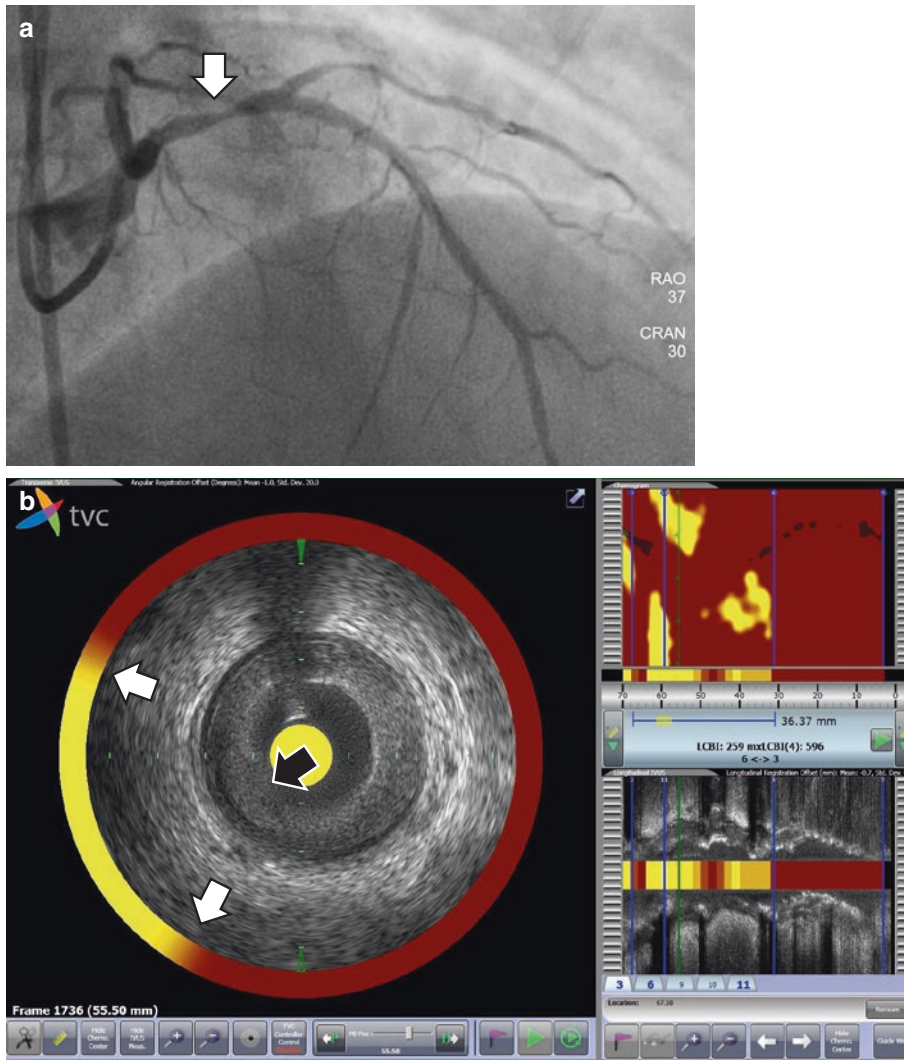

Fig. 9.1 Representative case of near-infrared spectroscopy (NIRS) in patient with acute coronary syndrome. The coronary angiogram shows significant stenosis at the proximal segment of the left anterior descending artery (*white arrow*) (**a**). NIRS shows large lipid burden within coronary artery wall (**b**). The cross-sectional image of NIRS clearly reveals lipid accumulation is present from 7 o'clock to 10 o'clock (*white arrow*), while concomitant intravascular ultrasound (IVUS) image demonstrates the presence of plaque rupture (*black arrow*) at the same location. In this case the identification of lipid by IVUS image is not feasible

9.2 Validation

NIRS system was rigorously validated with 84 human autopsy hearts in a prospective and double-blind manner to assess the accuracy in detecting the lipid core plaque (LCP) [4]. In order to develop quantitative index for the validation, an LCP of interest was defined as a lipid core >60° in circumferential extent, >200 μm thickness, and with a mean fibrous cap thickness <450 μm. The algorithm of NIRS system prospectively identified LCP with a receiver-operator characteristic area of 0.80 (95% confidence interval [CI]: 0.76–0.85). The lipid core burden index detected the presence or absence of any fibroatheroma with an area under the curve of 0.86 (95% CI: 0.81–0.91). This study successfully demonstrated good agreement between NIRS system and histopathology in coronary autopsy specimens. Clinical verification of NIRS system was performed by SPECTACL (Spectroscopic Assessment of Coronary Lipid) study. This study showed that spectral data obtained from patients by NIRS system were similar with those from autopsy specimens [5]. Furthermore, high reproducibility of NIRS system for the detection of LCP was demonstrated by Garcia et al. [6].

9.3 NIRS System and Measurement

NIRS system (TVC®, InfraReDx, Burlington, MA, USA) consists of 3.2F catheter, which uses 0.014-in. coronary guidewire system and pullback devices (Fig. 9.2). Mechanical pullback and rotation are performed at a speed of 0.5 cm/s and 240 rotation/m. The NIRS system acquires approximately 1000 NIRS measurement/12.5 cm of artery scanned and determines the presence of

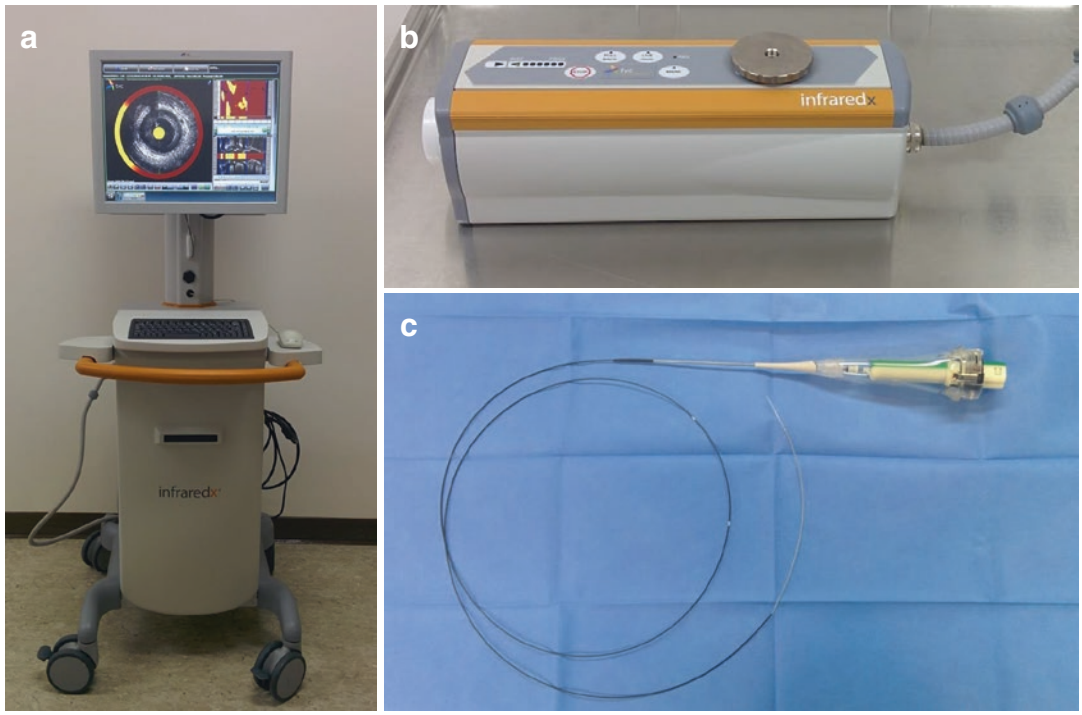

Fig. 9.2 Near-infrared (NIR) spectroscopy system (TVC®, InfraReDx, Burlington, MA, USA). The system consists of a console (**a**), a mechanical rotation pullback device (**b**), and a 3.2F imaging catheter (**c**). The disposable imaging catheter uses traditional 0.014-in. monorail system and contains an optical fiber to deliver NIR light from a console as well as intravascular ultrasound (IVUS) imaging system. The console integrates NIR information with IVUS image using predictive algorithm

lipid core plaque (LCP) at each interrogated location in the artery using a predictive algorithm. The calculated data are displayed in a two-dimensional map of the vessel ("chemogram") (Fig. 9.3a). The x-axis of the chemogram represents pullback position in millimeter scale, and the y-axis represents circumferential position in degrees (0–360°); a color scale from red to yellow indicates increasing probability that a LCP is present.

The block chemogram is a summary measurement of the probability that a LCP of 2-mm pullback interval is analyzed and displayed in a color map (Fig. 9.3b). The block chemogram uses the same color scale as the chemogram, but the display is summed up to four discrete colors to facilitate visual interpretation (red, $p < 0.57$; orange, $0.57 \leq p \leq 0.84$; tan, $0.84 \leq p \leq 0.98$; yellow, $p > 0.98$, algorithm probability that a LCP is present in that 2-mm block). Lipid core burden index (LCBI) is defined as the fraction of valid pixel in the chemogram that exceed a LCP probability of 0.6, multiplied by 1000 (Fig. 9.4). LCBI provides a summary measurement of the LCP presence in the entire scanned segment. The $\text{maxLCBI}_{4\text{mm}}$ is defined as the maximum value of LCBI for any of the 4-mm segment in the interrogated region and used as the index representing the size of the LCP (Fig. 9.5).

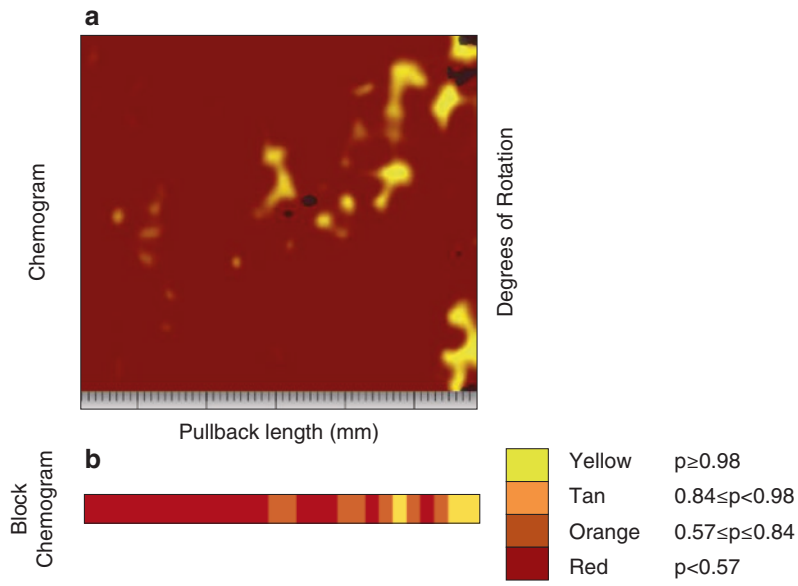

Fig. 9.3 An example of chemogram and block chemogram. (**a**) The color of chemogram from red to yellow indicates the increasing probability that a lipid core plaque (LCP) is present at this location. (**b**) Each color of the block chemogram is determined by 90th percentile value of the chemogram within a 2-mm segment. Four colors of the block chemogram represent chance of a LCP at this location (*red*, $p < 0.57$; *orange*, $0.57 \leq p \leq 0.84$; *tan*, $0.84 \leq p < 0.98$; *yellow*, $p \geq 0.98$)

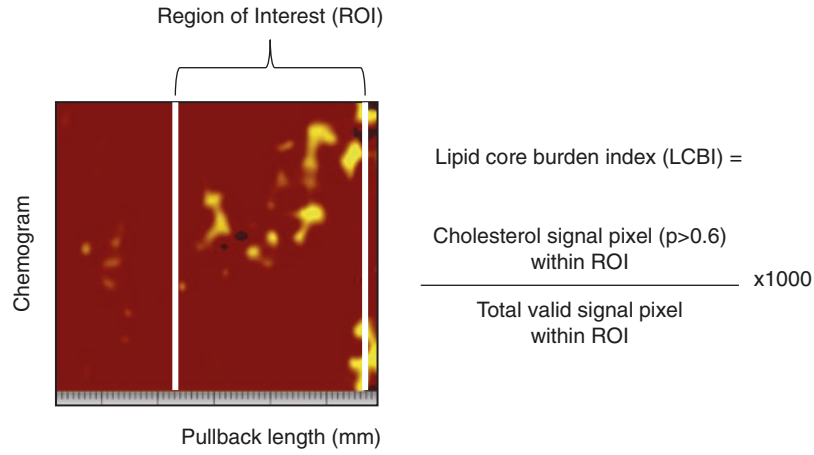

Fig. 9.4 Lipid core burden index (LCBI). LCBI is defined as cholesterol-positive signals which exceed an LCP probability of 0.6 within the region of interest divided by total valid signals multiplied by 1000 (‰)

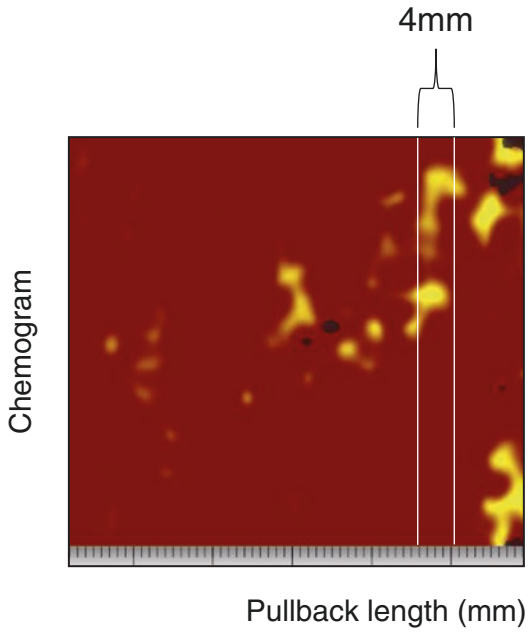

Fig. 9.5 maxLCBI4mm. maxLCBI4mm is defined as the maximum value of lipid core burden index for any of the 4-mm segment. It represents the angular size of the LCP

9.4 Clinical Studies

9.4.1 Prediction of Periprocedural MI

NIRS is able to identify high risk of periprocedural myocardial infarction (MI). Goldstein JA et al. observed 62 patients with stable cardiac biomarker who underwent coronary stenting [7]. Periprocedural MI was observed in 50% of patients with a maxLCBI4mm ≥ 500. On the other hand, periprocedural MI occurred only in 4.2% of patients with maxLCBI4mm < 500 ($p = 0.0002$). Quantification of LCP measured as maxLCBI4mm ≥ 500 was associated with increased risk of periprocedural MI, which is completely in accordance with traditional studies with IVUS or virtual histology (Fig. 9.6). The CANARY (Coronary Assessment by NIR of Atherosclerotic Rupture-Prone Yellow) study [8] enrolled 85 stable angina patients in a prospective and multicenter manner. NIRS performed prior to PCI

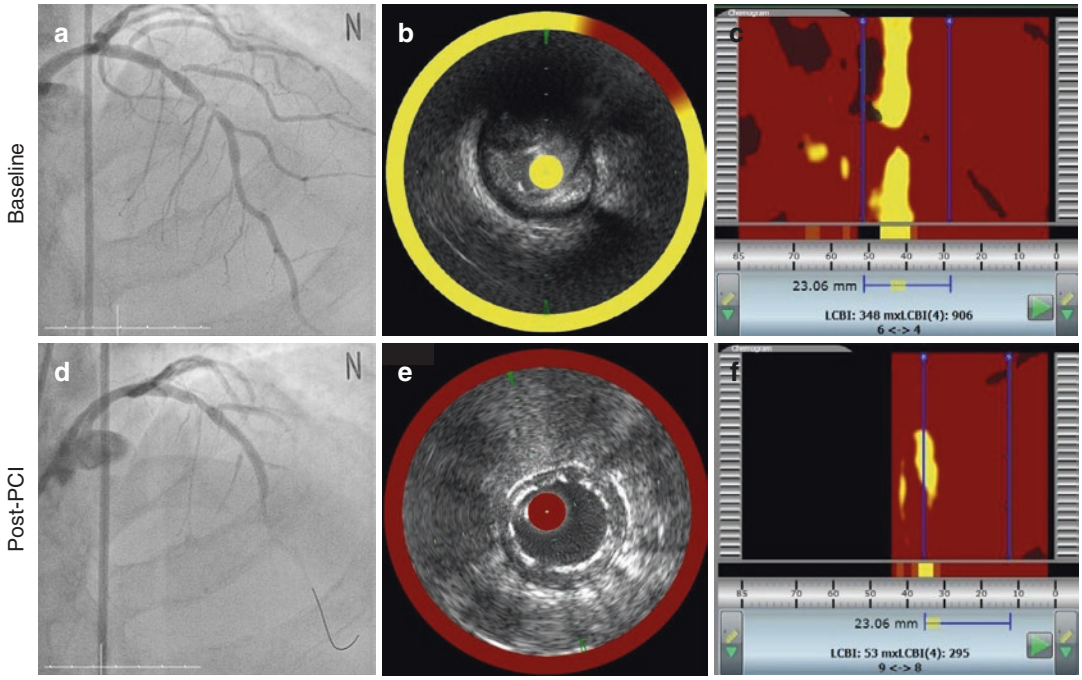

Fig. 9.6 Representative case of periprocedural myocardial infarction (MI) predicted by near-infrared spectroscopy. (**a**) Baseline angiogram shows discrete tight stenosis at the middle segment of the *left* anterior descending artery. (**b**) Baseline intravascular ultrasound (IVUS) shows significantly narrowed lumen with 1.75 mm^2 of minimal lumen area due to a large eccentric echo-attenuated plaque. The plaque burden was 86.9%. (**c**) The baseline chemogram displays "yellow" lipid-rich plaque extending almost 330° of the vessel circumference with maxLCBI4mm 906 (between *blue* lines), which highly suggests the development of periprocedural MI or no-reflow phenomenon. (**d**) Post-PCI angiogram shows no-reflow phenomenon. Cardiac biomarkers taken after the procedure were significantly elevated. (**e**) Post-PCI IVUS shows multiple stent struts well expanded and opposed to the vessel wall. Final minimal stent area is 5.8 mm^2. (**f**) The post-PCI chemogram displays significantly reduced and partly relocated lipid core area (*yellow*) after stenting. The maxLCBI4mm is 295 (between *blue* lines)

showed maxLCBI4mm was significantly higher (481.5 vs. 371.5, $p = 0.05$). However, among the randomized lesions with maxLCBI4mm ≥600, there was no difference of periprocedural MI with vs. without the use of distal protection filter (35.7% vs. 23.5%, respectively; relative risk, 1.52; 95% confidence interval: 0.50–4.60, $p = 0.69$). It is unclear whether this result is due to the limitation of NIRS predicting periprocedural MI or that of distal protection device preventing periprocedural MI. Further investigations will be needed to clarify this issue.

9.4.2 PCI Guidance

Visual assessment of coronary angiogram is commonly used to determine stent length. However, in terms of full lesion coverage, it is frequently inaccurate. IVUS can provide us more precise information than angiogram on lesion length by showing intravascular plaque morphology. Further, NIRS system substantiates another potential that it can give us additional information by showing the extent of lipid within coronary artery wall. Dixon et al. [9] observed that LCP extended beyond the angiographic margin of the lesion in 16% of PCI lesions. Whether LCP extending beyond the stent edges produces adverse outcome is unclear and requires further investigation. However, it is not difficult to expect that incomplete lesion coverage may increase the risk of stent edge problems such as restenosis requiring additional PCI or myocardial infarction. Strategy of PCI optimization with NIRS currently may be implicative.

9.4.3 Prediction of Outcome

Prospective identification of both vulnerable plaque and patient has been an important issue. However, only a small number of prospective outcome studies (Table 9.2), which assessed non-culprit lesions with intravascular imaging modalities, have been available. Most of them used IVUS or virtual histology (VH-IVUS) and have been describing several well-established features of vulnerable plaque (Table 9.2). Now accumulating data suggest that NIRS can identify vulnerable or rupture-prone plaque and predict outcome of the patients. Madder et al. reported maxLCBI4mm was 5.8-fold higher in STEMI culprit segments than in non-culprit segments of the STEMI culprit vessel (median [interquartile range (IQR)]: 523 [445–821] vs. 90 [6–265]; $p < 0.001$) [15]. A threshold of maxLCBI4mm ≥400 distinguished STEMI culprit (sensitivity, 85%; specificity, 98%). Oemrawsingh RM et al. observed non-culprit coronary arteries in 203 patients who were referred for coronary angiography [14]. About half (46%) of the patients had acute coronary syndrome. A four-fold increase in major adverse cardiac and cerebrovascular events during 1-year follow-up was observed in patients with LCBI above the median (16.7% vs. 4.0% event rate [adjusted hazard ratio, 4.04; 95% confidence interval, 1.33–12.29; $p = 0.01$]). Furthermore, the majority of event in this study was unplanned revascularization, which suggest NIRS is able to identify "active phase" or "rapid growing" plaque as well as rupture-prone plaque. Similarly, Madder et al. reported that in their 121 registry patients analysis maxLCBI4mm ≥400 in a non-stented segment at baseline is significantly associated with

Table 9.2 Imaging predictors in non-culprit lesion for clinical outcomes

Study	Patients	Method	Outcome	Results
Ohtani et al. [10]	552 pts	Angioscopy	7.1% ACS events at 57.3 ± 22.1-month FU	Number of yellow plaques (adjusted HR1.23[1.03–1.45], $p = 0.02$)
Prospect Stone et al. [11]	697 ACS pts	3-vessel VH-IVUS	11.6% MACE (cardiac death, cardiac arrest, MI, or rehospitalization) at 3.4-year FU	PB ≥ 70% (HR 5.03[2.51–10.11], $p < 0.001$), MLA ≤ 4.0 mm^2 (HR3.21[1.61–6.42], $p = 0.001$), VH-TCFA (HR3.35[1.77–6.36], $p < 0.001$)
Calvert et al. [12]	931 non-culprit lesions in 170 pts (41% ACS)	3-vessel VH-IVUS	1.4% MACE (death, MI, or unplanned revascularization) at 625-day FU	VH-TCFA (HR7.53, $p = 0.038$) and PB > 70% (HR 8.13, $p = 0.011$) remodeling index (HR2686 [1.94–3.72×10], $p = 0.032$)
Atheroremo-IVUS Cheng et al. [13]	581 pts (54% ACS)	VH-IVUS	7.8% MACE (mortality, ACS, or unplanned revascularization) at 1-year FU	VH-TCFA (adjusted HR1.98[1.09–3.60], $p = 0.026$) PB ≥ 70% (adjusted HR2.90[1.15–5.49], $p = 0.021$)
Atheroremo-NIRS Oemrawsingh et al. [14]	203 pts (47% ACS)	1-vessel NIRS	13.7% MACE (all-cause mortality, nonfatal ACS, stroke, and unplanned revascularization) at1-year FU	LCBI ≥ 43.0 (median) (adjusted HR4.04[1.33–12.29], $p = 0.01$)

ACS acute coronary syndrome, *FU* follow-up, *HR* hazard ratio, *pts* patients, *VH-IVUS* virtual histology intravascular ultrasound, *MACE* major adverse cardiac event, *MI* myocardial infarction, *PB* plaque burden, *MLA* minimal luminal area, *VH-TCFA* virtual histology thin-capped fibroatheroma, *NIRS* near-infrared spectroscopy, *LCBI* lipid core burden index

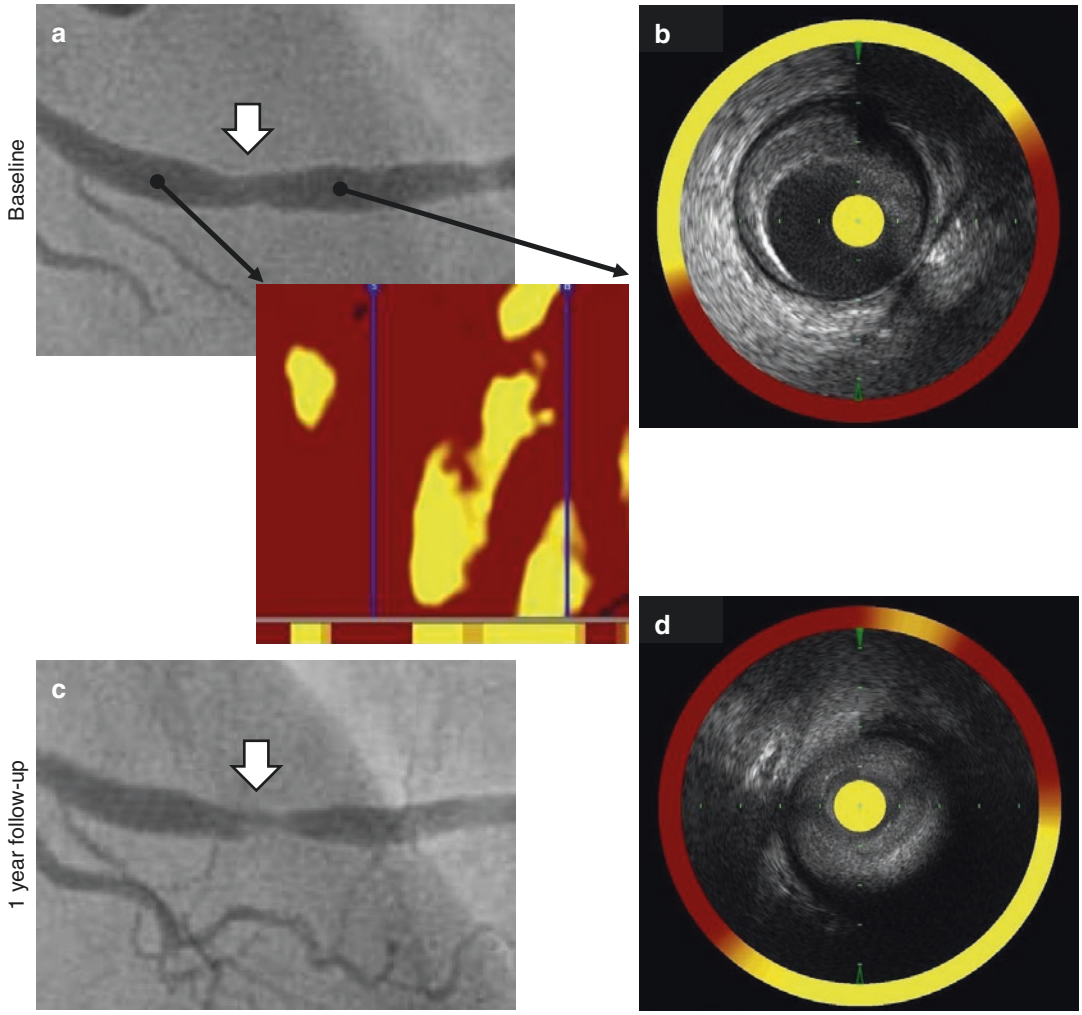

Fig. 9.7 Representative case of plaque progression predicted by near-infrared spectroscopy (NIRS). (**a**) Baseline angiogram shows insignificant stenosis (*white arrow*) at the middle segment of the *right* coronary artery. Concomitant NIRS scan displays the presence of large lipid core in the coronary artery wall (maxLCBI4mm is 483), which highly suggest the future cardiac event. (**b**) Baseline intravascular ultrasound (IVUS) shows an eccentric plaque with 8.2 mm^2 of minimal lumen area (MLA). The plaque burden is 58%. (**c**) The 1-year follow-up coronary angiogram shows definite "progression of plaque" with significant luminal narrowing (*white arrow*). (**d**) Follow-up IVUS shows narrowing of MLA (2.1 mm) and increased plaque burden (88%) compared with baseline images

adverse cardiac events during follow-up (HR 10.2, 95%CI 3.4–30.6, $P < 0.001$) [16]. NIRS is able to predict outcome in patients with coronary artery disease (Fig. 9.7).

9.4.4 Endothelial Dysfunction

Although the mechanism of exacerbating atherosclerosis by endothelial dysfunction has been extensively investigated in vitro and animal studies, in vivo demonstration using intravascular imaging technique such as IVUS has failed to substantiate this association. Choi B et al. reported that there was a significant correlation between LCBI ($r = -0.460$, $p = 0.008$), LCBI divided by lesion length ($r = -0.453$, $p = 0.009$), and maxLCBI4mm ($r = -0.431$, $p = 0.014$) and the degree of epicardial endothelial function [17]. NIRS system was sensitive enough to

detect the early changes of atherosclerosis according to the degree of endothelial dysfunction, which suggest it may serve as an important tool for assessing atherosclerosis and pathogenic mechanism of it.

9.5 Limitation

The NIRS system only provides two-dimensional information of cholesterol accumulation and does not provide information on the depth of the cholesterol within the coronary artery wall. IVUS may therefore be used for additional evaluation of plaque structure. False-positive reading of NIRS could be caused by fibroatheromas too small or with caps too thick to meet criteria for the LCP of interest or by lesions containing significant lipid but not having necrotic core (intimal xanthoma and pathologic intimal thickening).

Conclusion

The new lipid-identification methodology with NIR spectroscopy seems to be of value to research as well as clinical decision-making. Initial studies successfully demonstrated its ability and potentials. Several ongoing clinical trials may confirm its clinical usefulness and future applications.

References

1. Moreno PR, Muller JE. Identification of high-risk atherosclerotic plaques: a survey of spectroscopic methods. Curr Opin Cardiol. 2002;17:638–47.
2. Hall JW, Pollard A. Near-infrared spectrophotometry: a new dimension in clinical chemistry. Clin Chem. 1992;38:1623–31.
3. Caplan JD, Waxman S, Nesto RW, Muller JE. Near-infrared spectroscopy for the detection of vulnerable coronary artery plaques. J Am Coll Cardiol. 2006;47:C92–6.
4. Gardner CM, Tan H, Hull EL, Lisauskas JB, Sum ST, Meese TM, Jiang C, Madden SP, Caplan JD, Burke AP, Virmani R, Goldstein J, Muller JE. Detection of lipid core coronary plaques in autopsy specimens with a novel catheter-based near-infrared spectroscopy system. JACC Cardiovasc Imaging. 2008;1:638–48.
5. Waxman S, Dixon SR, L'Allier P, Moses JW, Petersen JL, Cutlip D, Tardif JC, Nesto RW, Muller JE, Hendricks MJ, Sum ST, Gardner CM, Goldstein JA, Stone GW, Krucoff MW. In vivo validation of a catheter-based near-infrared spectroscopy system for detection of lipid core coronary plaques: initial results of the SPECTACL study. JACC Cardiovasc Imaging. 2009;2:858–68.
6. Garcia BA, Wood F, Cipher D, Banerjee S, Brilakis ES. Reproducibility of near-infrared spectroscopy for the detection of lipid core coronary plaques and observed changes after coronary stent implantation. Catheter Cardiovasc Interv. 2010;76:359–65.
7. Goldstein JA, Maini B, Dixon SR, Brilakis ES, Grines CL, Rizik DG, Powers ER, Steinberg DH, Shunk KA, Weisz G, Moreno PR, Kini A, Sharma SK, Hendricks MJ, Sum ST, Madden SP, Muller JE, Stone GW, Kern MJ. Detection of lipid-core plaques by intracoronary near-infrared spectroscopy identifies high risk of periprocedural myocardial infarction. Circ Cardiovasc Interv. 2011;4:429–37.
8. Stone GW, Maehara A, Muller JE, Rizik DG, Shunk KA, Ben-Yehuda O, Genereux P, Dressler O, Parvataneni R, Madden S, Shah P, Brilakis ES, Kini AS, Investigators C. Plaque characterization to inform the prediction and prevention of periprocedural myocardial infarction during percutaneous coronary intervention: the CANARY trial (coronary assessment by near-infrared of atherosclerotic rupture-prone yellow). JACC Cardiovasc Interv. 2015;8:927–36.
9. Dixon SR, Grines CL, Munir A, Madder RD, Safian RD, Hanzel GS, Pica MC, Goldstein JA. Analysis of target lesion length before coronary artery stenting using angiography and near-infrared spectroscopy versus angiography alone. Am J Cardiol. 2012;109:60–6.
10. Ohtani T, Ueda Y, Mizote I, Oyabu J, Okada K, Hirayama A, Kodama K. Number of yellow plaques detected in a coronary artery is associated with future risk of acute coronary syndrome: detection of vulnerable patients by angioscopy. J Am Coll Cardiol. 2006;47:2194–200.
11. Stone GW, Maehara A, Lansky AJ, de Bruyne B, Cristea E, Mintz GS, Mehran R, McPherson J, Farhat N, Marso SP, Parise H, Templin B, White R, Zhang Z, Serruys PW, Investigators P. A prospective natural-history study of coronary atherosclerosis. N Engl J Med. 2011;364:226–35.
12. Calvert PA, Obaid DR, O'Sullivan M, Shapiro LM, McNab D, Densem CG, Schofield PM, Braganza D, Clarke SC, Ray KK, West NE, Bennett MR. Association between IVUS findings and adverse outcomes in patients with coronary artery disease: the VIVA (VH-IVUS in vulnerable atherosclerosis) study. JACC Cardiovasc Imaging. 2011;4:894–901.
13. Cheng JM, Garcia-Garcia HM, de Boer SP, Kardys I, Heo JH, Akkerhuis KM, Oemrawsingh RM, van Domburg RT, Ligthart J, Witberg KT, Regar E, Serruys PW, van Geuns RJ, Boersma E. In vivo detection of high-risk coronary plaques by radiofrequency intravascular ultrasound and cardiovascular outcome: results of the ATHEROREMO-IVUS study. Eur Heart J. 2014;35:639–47.

14. Oemrawsingh RM, Cheng JM, Garcia-Garcia HM, van Geuns RJ, de Boer SP, Simsek C, Kardys I, Lenzen MJ, van Domburg RT, Regar E, Serruys PW, Akkerhuis KM, Boersma E, Investigators A-N. Near-infrared spectroscopy predicts cardiovascular outcome in patients with coronary artery disease. J Am Coll Cardiol. 2014;64:2510–8.
15. Madder RD, Goldstein JA, Madden SP, Puri R, Wolski K, Hendricks M, Sum ST, Kini A, Sharma S, Rizik D, Brilakis ES, Shunk KA, Petersen J, Weisz G, Virmani R, Nicholls SJ, Maehara A, Mintz GS, Stone GW, Muller JE. Detection by near-infrared spectroscopy of large lipid core plaques at culprit sites in patients with acute ST-segment elevation myocardial infarction. JACC Cardiovasc Interv. 2013;6:838–46.
16. Madder RD, Husaini M, Davis AT, VanOosterhout S, Khan M, Wohns D, McNamara RF, Wolschleger K, Gribar J, Collins JS, Jacoby M, Decker JM, Hendricks M, Sum ST, Madden S, Ware JH, Muller JE. Large lipid-rich coronary plaques detected by near-infrared spectroscopy at non-stented sites in the target artery identify patients likely to experience future major adverse cardiovascular events. Eur Heart J Cardiovasc Imaging. 2016;17:393–9.
17. Choi BJ, Prasad A, Gulati R, Best PJ, Lennon RJ, Barsness GW, Lerman LO, Lerman A. Coronary endothelial dysfunction in patients with early coronary artery disease is associated with the increase in intravascular lipid core plaque. Eur Heart J. 2013;34:2047–54.